1.5 μm Lasers with Sub-10 mHz Linewidth

D. G. Matei,[1,*] T. Legero,[1] S. Häfner,[1] C. Grebing,[1,†] R. Weyrich,[1] W. Zhang,[2] L. Sonderhouse,[2] J. M. Robinson,[2] J. Ye,[2] F. Riehle,[1] and U. Sterr[1]

[1]*Physikalisch-Technische Bundesanstalt, Bundesallee 100, 38116 Braunschweig, Germany*

[2]*JILA, National Institute of Standards and Technology and University of Colorado, Department of Physics, 440 UCB, Boulder, Colorado 80309, USA*

(Received 14 February 2017; published 28 June 2017)

We report on two ultrastable lasers each stabilized to independent silicon Fabry-Pérot cavities operated at 124 K. The fractional frequency instability of each laser is completely determined by the fundamental thermal Brownian noise of the mirror coatings with a flicker noise floor of 4×10^{-17} for integration times between 0.8 s and a few tens of seconds. We rigorously treat the notorious divergences encountered with the associated flicker frequency noise and derive methods to relate this noise to observable and practically relevant linewidths and coherence times. The individual laser linewidth obtained from the phase noise spectrum or the direct beat note between the two lasers can be as small as 5 mHz at 194 THz. From the measured phase evolution between the two laser fields we derive usable phase coherence times for different applications of 11 to 55 s.

DOI: 10.1103/PhysRevLett.118.263202

It is well known that frequency is the physical quantity that can be measured with by far the highest accuracy. "Never measure anything but frequency!" was the advice of Arthur Schawlow [1]. The high accuracy results from the fact that the phase of a purely periodic signal can be measured in the simplest case by counting the zero crossings of the signal within a given time or with even increased accuracy by a phase measurement that interpolates the signal between the zero crossings. Hence, the generation of truly phase coherent signals over long times is the key to precision measurements and enabling technologies. In the most advanced optical atomic clocks [2–5], prestabilized lasers serve as oscillators to interrogate ultranarrow optical transitions with linewidths of a few mHz. Oscillators with coherence times of tens to hundreds of seconds will allow for investigations of extremely small energy shifts in the clock transition, caused by sources such as interactions amongst atoms [6,7]. Ultrastable oscillators beyond the state of the art will find useful applications in sub-mm very long baseline interferometry (VLBI) [8], atom interferometry and future atom-based gravitational wave detection [9–11], novel radar applications [12], the search for dark matter [13], and deep space navigation [14]. Consequently, great effort has been put into the development of extremely coherent sources based on highly stable optical Fabry-Pérot resonators [15–18]. Alternative schemes are currently being investigated using cavity-QED systems [17,19] and spectral-hole burning in cryogenically cooled crystals [20].

Here we report on the coherence properties of two cavity-stabilized laser systems operating at a wavelength of 1542 nm. Our systems are based on well-isolated single-crystal silicon Fabry-Pérot resonators, temperature stabilized at 124 K. For a system that has well-designed locking electronics, the fractional frequency stability of the laser is given by the fractional stability of the optical length of the cavity. Fundamentally, the cavities' length stability is limited by statistical Brownian noise of the mirror coatings, substrates, and spacer [21]. Because of the inherently low thermal noise of crystalline silicon, the cavities' length fluctuations are dominated by the dielectric mirror coatings, despite their thickness of only a few tens of micrometers. The cryogenic cooling of the cavities further reduces the thermal noise and allows for a fractional length instability of the cavities of $\Delta L/L \approx 10^{-17}$.

Previously, with such a system (named Si1) we demonstrated a frequency instability of 1×10^{-16} [15]. We have now set up two systems (named Si2 and Si3) where we have reduced all additional noise sources [22] to a level well below the thermal noise limit.

In the following we describe briefly the setup [23] and the analysis of the frequency stability and the phase noise. We subsequently derive methods to relate the dominant flicker frequency noise to observable and practically relevant linewidths and coherence times.

Each cavity consists of a plano-concave mirror pair employing high-reflectivity Ta_2O_5/SiO_2 dielectric multilayers. The finesse of the TEM_{00} mode of each cavity is close to 500 000. The 212 mm long spacer and the mirror substrates are machined from single-crystal silicon [15]. The crystal orientation of the optically contacted substrates is aligned to that of the spacer. Both have the silicon $\langle 111 \rangle$ axis oriented along the cavity axis.

The cavities are aligned vertically and are supported at three points near the midplane in order to minimize the impact of seismic and acoustic vibrations on their length stability. The anisotropic elasticity of silicon was

used to minimize the vertical vibration sensitivity below $10^{-12}/(\mathrm{m\,s^{-2}})$ by adjusting the azimuthal angle between the cavity and its tripod support [22].

The cavities are placed in separate vacuum systems at a residual pressure below 10^{-9} mbar. The cavity temperature is stabilized to 124 K where a zero crossing of the coefficient of thermal expansion of silicon occurs [15,22]. Each system is mounted on separate optical tables, about 3 m apart. The systems have their own active vibration isolation platforms and are surrounded by individual acoustic and temperature insulation boxes. They strongly suppress individual and thus also common noise contributions to below the thermal noise level on time scales up to several minutes [22].

Commercial Er-doped distributed feedback (DFB) fiber lasers at 1542 nm ($\nu_0 = 194.4$ THz) are frequency stabilized to the cavities using the Pound-Drever-Hall (PDH) method [26]. Fiber-coupled acousto-optic modulators (AOMs) are used for the fast servo allowing locking bandwidths of around 150 kHz. Active residual amplitude modulation (RAM) cancellation [27] is employed to keep the corresponding fractional frequency fluctuations below the thermal noise level of the system [22].

To obtain the individual frequency instabilities of the Si2 and Si3 lasers, we compared them to a third ultrastable laser based on a 48-cm-long ultralow expansion glass (ULE) cavity at 698 nm [16]. The frequency gap between the 1.5 μm Si2 system and the 698 nm ULE-cavity laser was bridged using a fiber-based optical frequency comb as a transfer oscillator [28,29]. The comb introduces negligible noise that is below the thermal noise floor of the ULE cavity. Additional noise arising from the optical fibers connecting the lasers and the frequency comb is suppressed with active noise cancellation [30].

We measured the beat frequencies "Si2—Si3" and "Si2—ULE" using synchronized counters [31]. The third beat frequency "Si3—ULE" is calculated as their difference which is justified since our beat measurement system does not introduce appreciable additional noise.

We do not expect correlations between the ULE-cavity system, the optical frequency comb, and the Si systems, since they reside in three different rooms. Thus, the three difference frequencies allowed us to derive the three individual instabilities from a simple three-cornered hat analysis [32] (Fig. 1). The relative linear frequency drift between Si2 and Si3 of about 100 μHz/s (comparable with the figure reported in Ref. [33]) and between Si2 and the ULE-cavity laser of 15 mHz/s is removed.

The three-cornered hat results (Fig. 1) [40] indicate that for averaging times from 0.8 s up to 10 s the instability of each Si-based laser system is at the expected thermal noise flicker floor of mod $\sigma_y = 4 \times 10^{-17}$. This corresponds to a standard Allan deviation of about 5×10^{-17} [46]. For short averaging times, the increase in the instability is due to residual vibration and acoustic noise. At long averaging times we see the effect

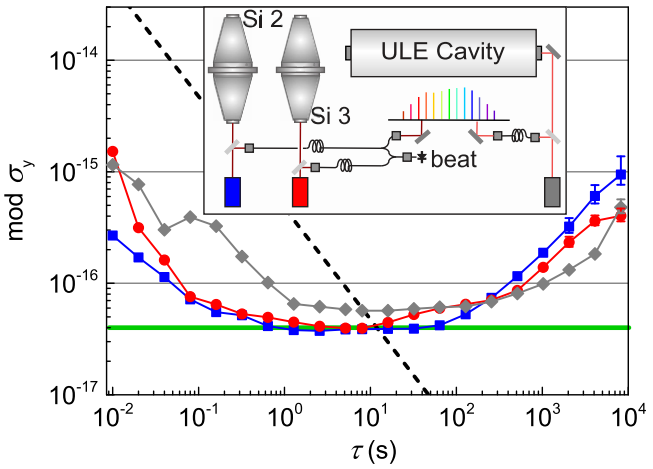

FIG. 1. Modified Allan deviation for Si2 (squares), Si3 (circles), and the ULE-cavity laser (diamonds) derived from three-cornered hat estimations. We used a 3.4 h data set for 10 ms $\leq \tau \leq$ 4 s and a 24.2 h data set for 8 s $\leq \tau \leq$ 8192 s, recorded in the same day. The green line represents the expected thermal noise of the silicon cavities. The dashed line illustrates the instability where the rms phase fluctuations are 1 rad for a given τ [34]. The intersections with the instability curves of the Si lasers result in coherence times of around 11 s. Linear frequency drifts in each data set were subtracted. The inset shows a schematic of the measurement setup.

of slow temperature fluctuations affecting the cavity length and of parasitic etalons in the optical setup.

A more complete characterization of the noise processes is given by the power spectral density (PSD) of the phase fluctuations. We have determined the phase of the beat signal from the measured in-phase and quadrature signal components. From more than 37 h of phase data we determine the phase noise spectrum of a single laser down to Fourier frequencies of 0.1 mHz (Fig. 2), modeled as

$$S_\phi(f) = \nu_0^2 \sum_{k=-2}^{0} h_k f^{k-2}. \quad (1)$$

From 1 mHz to 1 Hz, the noise spectrum closely follows the thermal frequency flicker noise with $h_{-1} = 1.7 \times 10^{-33}$, in agreement with the expected thermal noise. From 1 Hz to 3 kHz, the seismic and acoustic perturbations above the thermal noise lead to a number of narrow peaks. The base line of the spectrum can be approximated by white frequency noise with $h_0 = 3.6 \times 10^{-33}$ Hz^{-1} consistent with the increase of the instability at short averaging times (Fig. 1). Other possible sources such as photon shot-noise, RAM, and laser power fluctuations are well below that level. At higher frequencies, the three broad peaks at 8 kHz, 60 kHz, and 150 kHz result from the servo loops for RAM regulation, fiber noise cancellation, and PDH lock to the cavity, respectively. Below 1 mHz, slow temperature fluctuations lead to a random walk frequency noise with $h_{-2} = 4 \times 10^{-36}$ Hz, corresponding to the Allan deviation values above 100 s.

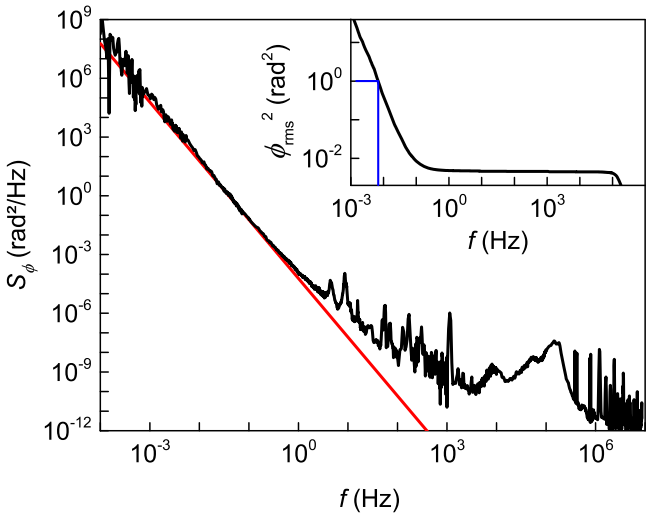

FIG. 2. PSD of phase fluctuations of a Si stabilized laser, obtained as one half of the PSD of the Si3—Si2 beat. The red line shows the expected flicker frequency noise corresponding to the thermal noise at $T = 124$ K. The inset shows the rms phase noise integrated down from 10 MHz. A value of 1 rad^2 is obtained after integrating down to 6.8 mHz (blue markers) leading to a FWHM linewidth of 13.6 mHz.

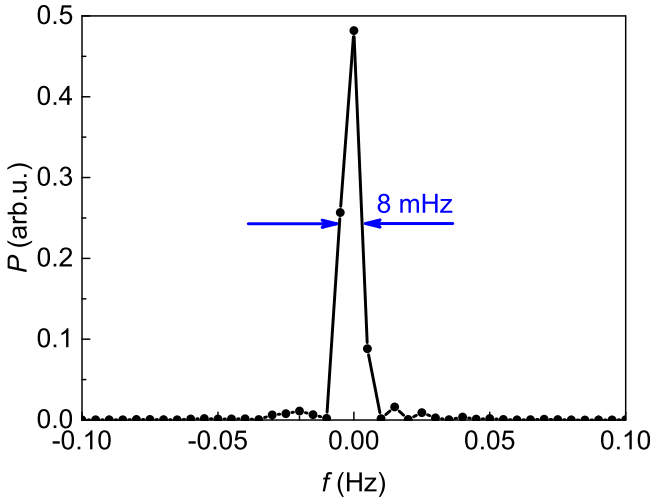

FIG. 3. FFT spectrum of the beat note between lasers Si2 and Si3 (Hanning window, frequency resolution 7.2 mHz).

In the following we use this data to derive values for laser linewidth and coherence time. Usually, linewidth and coherence time are derived from the autocorrelation function of the laser field with amplitude E_0 and center frequency ν_0,

$$R_E(\tau) = E_0^2 e^{i2\pi\nu_0\tau} e^{-1/2\langle(\phi(t+\tau)-\phi(t))^2\rangle}, \\ = E_0^2 e^{i2\pi\nu_0\tau} e^{-2\int_0^\infty S_\phi(f)\sin^2(\pi f\tau)df}. \quad (2)$$

Flicker frequency noise and random walk frequency noise are the dominant noise processes in our lasers. In this case, the laser frequency $\nu(t)$ is nonstationary and $R_E(\tau)$ is divergent so that no unique coherence function can be assigned. This also leads to divergences in the general definition of the field spectrum $S_E(\delta\nu)$ as the Fourier transform of the autocorrelation function $R_E(\tau)$ [Eq. (2)] and thus no uniquely defined linewidth exists. Nevertheless we can derive linewidths that are closely related to the experimental observations.

If a spectrum is recorded for a measurement time T_0 the linewidth is limited by the Fourier width proportional to $1/T_0$ for short measuring times whereas for longer measurement times the nonstationary frequency fluctuations broaden the line. In such a case a practical linewidth can be defined by the minimum.

To elaborate this approach Bishof *et al.* [18] make the assumption that only Fourier components of the phase noise spectrum for frequencies $f > 1/T_0$ contribute during the measurement time T_0. From our phase noise model [Eq. (1)] we obtain a minimal single laser linewidth of $\Delta\nu_{\mathrm{FWHM}} = 7$ mHz for $T_0 = 170$ s [47].

Experimentally we obtain linewidths from a fast Fourier transform (FFT) of the beat between the two lasers, after the beat is mixed down to a carrier frequency suitable for data acquisition. We choose 200 s measurement time to allow for sufficiently high frequency resolution while keeping the influence of slow frequency fluctuations small enough. Experimentally, in about 43% of the measurements [53] we obtain full-width-half-maximum (FWHM) linewidths of the beat signal between 7 mHz and 14 mHz (see Fig. 3), leading to individual linewidths $\Delta\nu_{\mathrm{FWHM}}$ between 5 mHz to 10 mHz, assuming that both lasers contribute equally to the linewidth. This standard approach of measuring the linewidth seems to give a reasonable agreement with the calculated minimal linewidth of 7 mHz according to Ref. [18].

To provide a linewidth estimate that includes all fluctuations of the flicker frequency noise, we averaged all FFT spectra obtained from the data set of 37 h after first aligning their centers of mass [53]. This results in an average linewidth for a single laser of about 13 mHz for a measurement time of 150 s. The difference between this long-term averaged value and the calculated minimal linewidth can be explained by the different ways the low-frequency cutoff is introduced. If a FFT spectrum analyzer is used, the spectrum is centered at the average frequency during the measurement time T_0 which corresponds to a subtraction of the linear phase evolution term. Thus significant quadratic terms still contribute to the phase excursion which correspond to noise at frequencies of approximately $1/2T_0$ that is not included in the approximation of Ref. [18]. The narrower linewidths that we have observed (Fig. 3) are cases where the random quadratic term happened to be small.

Many applications are not directly sensitive to the FWHM linewidth but require sufficient spectral power in a narrow bandwidth $\Delta\nu_{\mathrm{P}}$. This bandwidth can be estimated

by integrating the phase noise from high frequencies towards zero [54,55]. The half bandwidth is obtained as the lower integration limit in

$$\int_{\Delta\nu_P/2}^{\infty} S_\phi(f)df = 1 \text{ rad}^2, \quad (3)$$

corresponding to the case when one third of the power is contained in the bandwidth $\Delta\nu_P$ [55]. For this definition we find a value of $\Delta\nu_P = 14$ mHz (see inset of Fig. 2).

For many applications it is important to provide effective coherence times of ultrastable oscillators. For this purpose, depending on the particular application, different methods must be employed to adequately consider the nonstationary frequency.

As an example more adequate for optical clocks, we investigate a two-pulse Ramsey interrogation of atoms. There, an average frequency and frequency drift can be estimated from past measurements and considered in the current interrogation in order to keep the phase excursions $\Delta\phi$ between the two pulses sufficiently small.

We simulate such a scenario using the phase evolution of the Si2—Si3 beat recorded for 1 day. We cut this data set into short samples and fit a linear phase to the first 4 s (i.e., observation interval T_0) to determine the average frequency $\bar{\nu}$. The phase $2\pi\bar{\nu}t$ is subtracted and the phase at $t = 0$ is set to zero to obtain the phase deviation $\Delta\phi$ for $t \geq 0$. Figure 4 shows 100 of these samples, which indicate a time-dependent broadening. The root-mean-square deviation $\Delta\phi_{\text{rms}}(t)$ of the normally distributed phase deviation was calculated from 20 750 samples ($\pm\Delta\phi_{\text{rms}}$ indicated by red lines). The coherence is certainly lost when the phase has acquired an uncertainty of $\Delta\phi_{\text{rms}} \approx \pi$ (at $t \approx 30$ s) but depending on the application, more restricting definitions of the coherence time are in use. In a more conservative way we define the coherence time as a duration in which $\Delta\phi_{\text{rms}}$ has increased to 1 rad (i.e., $\sqrt{2}$ rad for the phase difference between the two independent lasers shown in Fig. 4). In agreement with the value estimated from the Allan deviation (Fig. 1) [34], this leads to a coherence time of 11 s. This is equivalent to saying that after 11 s in more than 99% of all cases the actual phase excursions remain below $\pm\pi \approx 3\Delta\phi_{\text{rms}}$, which ensures unambiguous phase tracing. We find that this value of 11 s represents a broad maximum in the coherence time when the Ramsey interrogation time varies between 4 s and 20 s [34].

Besides situations where the future phase must be predicted there are many applications where the average frequency can be determined in retrospect from the measurement itself. Typical examples are spectral analysis, when the spectrum is centered, or the Rabi interrogation of atoms by single pulses, where the observed excitation provides the information of the average frequency during the measurement time. Analysis of our measured phase data shows that in this case an rms phase deviation of $\Delta\phi_{\text{rms}} = 1$ rad occurs at measurement intervals of about 55 s [34].

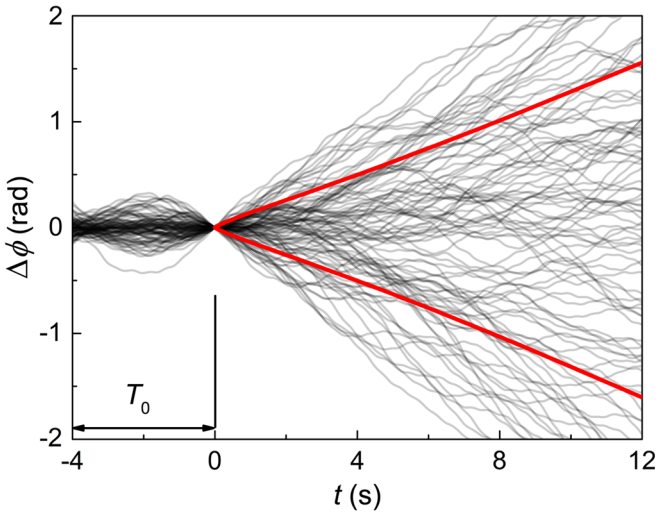

FIG. 4. The evolution of the phase difference between the two Si lasers. The first 4 s segment T_0 is used to estimate the average frequency $\bar{\nu}$ at $t = 0$ s. For $t = 0$–12 s, the phase deviation from the expected $2\pi\bar{\nu}t$ is calculated. 100 consecutive curves are shown with thin gray lines. The red lines indicate the $\pm\Delta\phi_{\text{rms}}$ range, evaluated statistically from 20 750 curves.

In conclusion, we have demonstrated the operation of two cryogenic optical silicon cavities at the thermal noise limit of mod $\sigma_y = 4 \times 10^{-17}$. The light stabilized on these cavities is highly coherent, with a coherence time of 11 s to 55 s. As seen from the spectral analysis, the linewidth and implicitly the coherence time are mostly determined by the thermal noise level. With this kind of laser sources we are now entering the regime where the frequency stability of the interrogation laser is on a par with the quantum projection noise limit of today's most stable optical clocks (e.g., [56,57]).

Optimizations of the current setup would hardly bring a longer coherence time since we are nearing a fundamental limit. The only way of further improving the current performance is to decrease the thermal noise even further. One approach is to decrease the temperature, thus reducing the thermal motion in the system. For an operating temperature of 4 K the expected thermal noise would be 8×10^{-18} in the modified Allan deviation. A comparable noise figure would be achieved by employing AlGaAs-based crystalline coatings, which offer a higher mechanical Q factor and thus a lower thermal-induced noise [58,59]. If both methods are implemented, the thermal noise would be reduced to the lower half of the 10^{-18} range, roughly an order of magnitude lower than the present level. To ensure that this improvement leads to an increased coherence time it is necessary to reduce the long-term instability for averaging times above 10 s (see intersection of dashed line with the thermal noise level in Fig. 1) while the present short-term instability seems to be sufficiently small.

Our rigorous analysis of linewidth and coherence time will be tremendously important when we start using this state-of-the-art laser, e.g., for investigations of classical and/or quantum correlated atoms [60]. Achieving enhanced stability from quantum correlation (such as spin squeezing) will need a local oscillator that does not introduce excessive phase noise which can easily remove the benefit of correlation [61].

This silicon cavity work is supported and developed jointly by the Centre for Quantum Engineering and Space-Time Research (QUEST), Physikalisch-Technische Bundesanstalt (PTB), the JILA Physics Frontier Center (NSF), the National Institute of Standards and Technology (NIST). This project has received funding under 15SIB03 OC18 from the EMPIR programme co-financed by the Participating States and from the European Union's Horizon 2020 research and innovation programme. We also acknowledge support by the European Metrology Research Programme (EMRP) under QESOCAS. The EMRP is jointly funded by the EMRP participating countries within EURAMET, and the European Union. We wish to thank U. Kuetgens and D. Schulze for x-ray orientation of the spacer and mirrors, and E. Oelker for helpful comments to the manuscript. J. Ye thanks the Alexander von Humboldt Foundation for support. L. Sonderhouse is supported by the National Defense Science and Engineering Graduate (NDSEG) fellowship.

*dan.matei@ptb.de
†Present address: TRUMPF Scientific Lasers GmbH+Co. KG, Feringastr. 10a, 85774 Unterföhring, Germany.

[1] T. W. Hänsch, Rev. Mod. Phys. **78**, 1297 (2006).
[2] A. D. Ludlow, M. M. Boyd, J. Ye, E. Peik, and P. O. Schmidt, Rev. Mod. Phys. **87**, 637 (2015).
[3] T. L. Nicholson, S. L. Campbell, R. B. Hutson, G. E. Marti, B. J. Bloom, R. L. McNally, W. Zhang, M. D. Barrett, M. S. Safronova, G. F. Strouse, W. L. Tew, and J. Ye, Nat. Commun. **6**, 6896 (2015).
[4] I. Ushijima, M. Takamoto, M. Das, T. Ohkubo, and H. Katori, Nat. Photonics **9**, 185 (2015).
[5] N. Huntemann, C. Sanner, B. Lipphardt, C. Tamm, and E. Peik, Phys. Rev. Lett. **116**, 063001 (2016).
[6] A. M. Rey, A. V. Gorshkov, C. V. Kraus, M. J. Martin, M. Bishof, M. D. Swallows, X. Zhang, C. Benko, J. Ye, N. D. Lemke, and A. D. Ludlow, Ann. Phys. (Amsterdam) **340**, 311 (2014).
[7] M. J. Martin, M. Bishof, M. D. Swallows, X. Zhang, C. Benko, J. von Stecher, A. V. Gorshkov, A. M. Rey, and J. Ye, Science **341**, 632 (2013).
[8] S. Doeleman, T. Mai, A. E. E. Rogers, J. G. Hartnett, M. E. Tobar, and N. Nand, Publ. Astron. Soc. Pac. **123**, 582 (2011).
[9] J. M. Hogan and M. A. Kasevich, Phys. Rev. A **94**, 033632 (2016).
[10] S. Kolkowitz, I. Pikovski, N. Langellier, M. D. Lukin, R. L. Walsworth, and J. Ye, Phys. Rev. D **94**, 124043 (2016).
[11] B. Canuel, S. Pelisson, L. Amand, A. Bertoldi, E. Cormier, B. Fang, S. Gaffet, R. Geiger, J. Harms, D. Holleville, A. Landragin, G. Lefèvre, J. Lhermite, N. Mielec, M. Prevedelli, I. Riou, and P. Bouyer, Proc. SPIE Int. Soc. Opt. Eng. **9900**, 990008 (2016).
[12] P. Ghelfi, F. Laghezza, F. Scotti, G. Serafino, A. Capria, S. Pinna, D. Onori, C. Porzi, M. Scaffardi, A. Malacarne, V. Vercesi, E. Lazzeri, F. Berizzi, and A. Bogoni, Nature (London) **507**, 341 (2014).
[13] A. Derevianko and M. Pospelov, Nat. Phys. **10**, 933 (2014).
[14] S. Grop, P. Y. Bourgeois, N. Bazin, Y. Kersalé, E. Rubiola, C. Langham, M. Oxborrow, D. Clapton, S. Walker, J. De Vicente, and V. Giordano, Rev. Sci. Instrum. **81**, 025102 (2010).
[15] T. Kessler, C. Hagemann, C. Grebing, T. Legero, U. Sterr, F. Riehle, M. J. Martin, L. Chen, and J. Ye, Nat. Photonics **6**, 687 (2012).
[16] S. Häfner, S. Falke, C. Grebing, S. Vogt, T. Legero, M. Merimaa, C. Lisdat, and U. Sterr, Opt. Lett. **40**, 2112 (2015).
[17] M. A. Norcia and J. K. Thompson, Phys. Rev. X **6**, 011025 (2016).
[18] M. Bishof, X. Zhang, M. J. Martin, and J. Ye, Phys. Rev. Lett. **111**, 093604 (2013).
[19] B. T. R. Christensen, M. R. Henriksen, S. A. Schäffer, P. G. Westergaard, D. Tieri, J. Ye, M. J. Holland, and J. W. Thomsen, Phys. Rev. A **92**, 053820 (2015).
[20] S. Cook, T. Rosenband, and D. R. Leibrandt, Phys. Rev. Lett. **114**, 253902 (2015).
[21] K. Numata, A. Kemery, and J. Camp, Phys. Rev. Lett. **93**, 250602 (2004).
[22] D. G. Matei, T. Legero, C. Grebing, S. Häfner, C. Lisdat, R. Weyrich, W. Zhang, L. Sonderhouse, J. M. Robinson, F. Riehle, J. Ye, and U. Sterr, J. Phys. Conf. Ser. **723**, 012031 (2016).
[23] See Supplemental Material at http://link.aps.org/supplemental/10.1103/PhysRevLett.118.263202 for the Section "Set-up: reduction of technical noise," which includes Refs. [24,25].
[24] T. Middelmann, A. Walkov, G. Bartl, and R. Schödel, Phys. Rev. B **92**, 174113 (2015).
[25] G. Rupschus, R. Niepraschk, K. Jousten, and M. Kühne, J. Vac. Sci. Technol., A **12**, 1686 (1994).
[26] R. W. P. Drever, J. L. Hall, F. V. Kowalski, J. Hough, G. M. Ford, A. J. Munley, and H. Ward, Appl. Phys. B **31**, 97 (1983).
[27] W. Zhang, M. J. Martin, C. Benko, J. L. Hall, J. Ye, C. Hagemann, T. Legero, U. Sterr, F. Riehle, G. D. Cole, and M. Aspelmeyer, Opt. Lett. **39**, 1980 (2014).
[28] H. R. Telle, B. Lipphardt, and J. Stenger, Appl. Phys. B **74**, 1 (2002).
[29] J. Stenger, H. Schnatz, C. Tamm, and H. R. Telle, Phys. Rev. Lett. **88**, 073601 (2002).
[30] L.-S. Ma, P. Jungner, J. Ye, and J. L. Hall, Opt. Lett. **19**, 1777 (1994).
[31] G. Kramer and W. Klische, in *Proceedings of the 18th European Frequency and Time Forum, Guildford, UK* (IET, London, UK, 2004), pp. 595–602.
[32] J. E. Gray and D. W. Allan, in *Proceedings of the 28th Annual Symposium on Frequency Control, 29-31 May*

1974, Atlantic City, New Jersey, New Jersey (Electronic Industries Association, Washington, D.C., 1974), pp. 243–246.
[33] C. Hagemann, C. Grebing, C. Lisdat, S. Falke, T. Legero, U. Sterr, F. Riehle, M. J. Martin, and J. Ye, Opt. Lett. **39**, 5102 (2014).
[34] See Supplemental Material at http://link.aps.org/supplemental/10.1103/PhysRevLett.118.263202 for the Section "Coherence time," which includes Refs. [35–39].
[35] B. E. A. Saleh and M. C. Teich, *Fundamentals of Photonics* (John Wiley & Sons, Inc., New York, New York, 1991).
[36] V. N. Mahajan, J. Opt. Soc. Am. **72**, 1258 (1982).
[37] W. Klemperer, Proc. IEEE **60**, 602 (1972).
[38] A. E. E. Rogers and J. M. Moran, Jr., IEEE Trans. Instrum. Meas. **IM-30**, 283 (1981).
[39] A. R. Thompson, J. M. Moran, and G. W. Swenson, *Interferometry and Synthesis in Radio Astronomy* (Wiley, New York, 2007).
[40] See Supplemental Material at http://link.aps.org/supplemental/10.1103/PhysRevLett.118.263202 for the Section "Allan deviation," which includes Refs. [41–45].
[41] C. Hagemann, C. Grebing, T. Kessler, S. Falke, N. Lemke, C. Lisdat, H. Schnatz, F. Riehle, and U. Sterr, IEEE Trans. Instrum. Meas. **62**, 1556 (2013).
[42] D. W. Allan and J. Barnes, in *Proceedings of the 35th Ann. Freq. Control Symposium* (Electronic Industries Association, Ft. Monmouth, NJ, 1981), pp. 470–475, for corrections see Ref. [43].
[43] D. Sullivan, D. Allan, D. Howe, and F. Walls, *Characterization of Clocks and Oscillators*, NIST Tech. Note 1337 (NIST, U.S Department of Commerce, National Institute of Standards and Technology, 1990), online available at http://tf.boulder.nist.gov/general/pdf/868.pdf.
[44] E. Benkler, C. Lisdat, and U. Sterr, Metrologia **52**, 565 (2015).
[45] E. Rubiola, Rev. Sci. Instrum. **76**, 054703 (2005).
[46] S. T. Dawkins, J. J. McFerran, and A. N. Luiten, IEEE Trans. Ultrason. Ferroelectr. Freq. Control **54**, 918 (2007).
[47] See Supplemental Material at http://link.aps.org/supplemental/10.1103/PhysRevLett.118.263202 for the Section "Spectral width calculations," which includes Refs. [48–52].
[48] D. W. Allan, IEEE Trans. Instrum. Meas. **IM-36**, 646 (1987).
[49] G. M. Stephan, T. T. Tam, S. Blin, P. Besnard, and M. Tetu, Phys. Rev. A **71**, 043809 (2005).
[50] F. J. Harris, Proc. IEEE **66**, 51 (1978).
[51] N. Von Bandel, M. Myara, M. Sellahi, T. Souici, R. Dardaillon, and P. Signoret, Opt. Express **24**, 27961 (2016).
[52] D. A. Steck, *Quantum and Atom Optics* [available online at http://steck.us/teaching (Revision 0.11.6, 24 February 2017)].
[53] See Supplemental Material at http://link.aps.org/supplemental/10.1103/PhysRevLett.118.263202 for the Section "FFT statistics".
[54] F. L. Walls and A. E. Wainwright, IEEE Trans. Instrum. Meas. **24**, 15 (1975).
[55] J. L. Hall and M. Zhu, in *Laser Manipulation of Atoms and Ions, Proceedings Internat. School of Physics Enrico Fermi, Vol. Course CXVIII* (North Holland-Elsevier, Amsterdam, 1992), pp. 671–702.
[56] M. Schioppo, R. C. Brown, W. F. McGrew, N. Hinkley, R. J. Fasano, K. Beloy, T. H. Yoon, G. Milani, D. Nicolodi, J. A. Sherman, N. B. Phillips, C. W. Oates, and A. D. Ludlow, Nat. Photonics **11**, 48 (2017).
[57] S. L. Campbell, R. B. Hutson, G. E. Marti, A. Goban, N. D. Oppong, R. L. McNally, L. Sonderhouse, J. M. Robinson, W. Zhang, B. J. Bloom, and J. Ye, arXiv:1702.01210.
[58] G. D. Cole, W. Zhang, M. J. Martin, J. Ye, and M. Aspelmeyer, Nat. Photonics **7**, 644 (2013).
[59] G. D. Cole, W. Zhang, B. J. Bjork, D. Follman, P. Heu, C. Deutsch, L. Sonderhouse, J. Robinson, C. Franz, A. Alexandrovski, M. Notcutt, O. H. Heckl, J. Ye, and M. Aspelmeyer, Optica **3**, 647 (2016).
[60] E. Paladino, Y. M. Galperin, G. Falci, and B. L. Altshuler, Rev. Mod. Phys. **86**, 361 (2014).
[61] E. M. Kessler, P. Kómár, M. Bishof, L. Jiang, A. S. Sørensen, J. Ye, and M. D. Lukin, Phys. Rev. Lett. **112**, 190403 (2014).